Ion-transporting capacity and aerobic respiration of larval white seabass (*Atractoscion nobilis*) may be resilient to ocean acidification conditions

Garfield T Kwan[1, 2*], Sara G Shen[1*†], Mark Drawbridge[3], David M Checkley, Jr. [1], Martin Tresguerres[1†]

[1] Scripps Institution of Oceanography, University of California, San Diego, La Jolla, CA, USA

[2] National Oceanic and Atmospheric Administration Fisheries Service, Southwest Fisheries Science Center, 8901 La Jolla Shores Drive, La Jolla, CA, 92037, USA

[3] Hubbs-SeaWorld Research Institute, San Diego, CA, USA

*These authors contributed equally to this work; †Corresponding authors

Keywords: ocean acidification, Na^+/K^+-ATPase, ionocyte, oxygen consumption, transgenerational acclimation, recirculating aquarium system

Abstract – 250 words currently

Ocean acidification (OA) has been proposed to increase the energetic demand for acid-base regulation at the expense of larval fish growth. Here, white seabass (*Atractoscion nobilis*) eggs and larvae were reared at control (542 ± 28 µatm) and elevated pCO_2 (1,831 ± 105 µatm) until five days post-fertilization (dpf). Skin ionocytes were identified by immunodetection of the Na^+/K^+-ATPase (NKA) enzyme. Larvae exposed to elevated pCO_2 possessed significantly higher skin ionocyte number and density compared to control larvae. However, when ionocyte size was accounted for, the relative ionocyte area (a proxy for total ionoregulatory capacity) was unchanged. Similarly, there were no differences in relative NKA abundance, resting O_2 consumption rate, and total length between control and treatment larvae at 5 dpf, nor in the rate at which relative ionocyte area and total length changed between 2–5 dpf. Altogether, our results suggest that OA conditions projected for the next century do not significantly affect the ionoregulatory capacity or energy consumption of larval white seabass. Finally, a retroactive analysis of the water in the recirculating aquarium system that housed the broodstock revealed the parents had been exposed to average pCO_2 of ~1,200 µatm for at least 3.5 years prior to this experiment. Future studies should investigate whether larval white seabass are naturally resilient to OA, or if this resilience is the result of parental chronic acclimation to OA, and/or from natural selection during spawning and fertilization in elevated pCO_2.

Research Highlights

- Larval white seabass were lab-exposed to elevated CO_2 levels simulating future ocean acidification (OA).
- Exposure to OA did not induce any changes in ion-transporting capacity, aerobic respiration rate, or total length of larval white seabass.

- Retroactive analysis of the water in broodstock tanks revealed the parents had been chronically exposed to elevated CO_2 levels, which may have affected the physiology of the larvae and conferred the observed resilience.

Introduction

The survival of fish during the early life stages is the serendipitous outcome of a favorable combination of oceanographic, hydrographic, climatic, biological, and trophodynamic factors (Houde, 2009). Without the ability to swim, fish eggs, embryos and pre-flexion larvae may be advected offshore to suboptimal habitat, consumed by zooplankton and other predators, or starve before finding suitable prey (Hjort, 1926; Houde, 2009). As a result of the environment's strong control over recruitment dynamics, mortality is high and variable during the vulnerable early life stages (Beaugrand et al., 2003; Houde, 2009). Of particular concern is the impacts of climate change on larval fish survival. Under 'business-as-usual' emission scenarios, the average partial pressure of carbon dioxide (pCO_2) in the global surface ocean is projected to reach ~1,000 µatm by the year 2100 and ~2,000 µatm by the year 2300, with a corresponding decrease in pH from current levels of ~8.0 down to ~7.7 and ~7.4 respectively (Caldeira and Wickett, 2003, 2005; Meehl et al., 2007; Goodwin et al., 2018; Bindoff et al., 2019). This phenomenon, "ocean acidification" (OA), may further challenge survival during the early life stages through disturbances to acid-base homeostasis leading to physiological, energetic, or behavioral alterations (Heuer and Grosell, 2014; Esbaugh, 2017; Tresguerres and Hamilton, 2017).

Many of the reported potentially negative effects of OA on fish larvae have been attributed to their lack of gill and their Na^+/K^+-ATPase-rich (NKA) ionocytes (e.g. Ishimatsu et al., 2008; Frommel et al., 2011; Baumann et al., 2012; Pimentel et al., 2014, 2015), the primary organ for blood acid-base regulation (reviewed in Evans et al., 2005). However, this explanation

dismisses the NKA-rich ionocytes found on the skin of embryonic and larval fishes (Varsamos et al., 2002; Dahlke et al., 2017, 2020; Kwan et al., 2019a; reviewed in Glover et al., 2013). As the larvae grow and their gills develop, the abundance of larval skin ionocyte decreases as the ion-transport requirements are increasingly fulfilled by the gill ionocytes (Ayson et al., 1994; Hiroi et al., 1998, 1999; Varsamos et al., 2002; Kwan et al., 2019a). Recently, the ion-transporting capacity of larval skin ionocytes has been shown to be comparable to that of their adult counterpart, the gill ionocytes (Dahlke et al., 2020). Yet despite their differences in spatial localization, both skin and gill ionocytes rely on basolateral NKA to generate an electrochemical gradient necessary for maintaining osmotic and acid-base homeostasis. As a result, the immunostaining and quantification of NKA-rich ionocytes on the larva's epithelial surface can serve as a useful proxy for the ion-transporting capacity and underlying energetic demand.

The few studies that have explored the effects of OA on larval fish ionocytes found no significant differences in skin density (Dahlke et al., 2017), NKA expression, or NKA activity (Dahlke et al., 2020). Nonetheless, the increased otolith size and neurobehavioral alterations observed during exposure to elevated pCO_2 indicate that both larval and adult fishes maintain blood pH homeostasis by excreting H^+ and accumulating HCO_3^- (reviewed in Tresguerres and Hamilton, 2017). This putative upregulation in acid-base homeostasis during OA exposure could entail increased energy consumption, which in turn could impair larval development and growth (Pimentel et al., 2014; Dahlke et al., 2017, 2020).

Basal energy consumption is commonly assessed through measurements of resting oxygen (O_2) consumption rate (rOCR) and somatic size (e.g. total length). Previous studies on the effects of OA on fish larvae reported diverse and variable results, with rOCR and body size increasing, decreasing, or remaining unchanged (Munday et al., 2009, 2016; Baumann et al., 2012; Miller et al., 2012; Bignami et al., 2013; Pimentel et al., 2014, 2015; Flynn et al., 2015; Rossi et al., 2015; Murray et al., 2016; Dahlke et al., 2017). As proposed in some of those studies, the variation in responses may be due to differences in pCO_2/pH exposure levels,

duration, or unidentified species-specific physiological mechanisms that determined their differential vulnerability to OA. In addition, some studies have suggested the possibility of transgenerational acclimation (Miller et al., 2012; Munday, 2014; Murray et al., 2014; Cattano et al., 2016; Stiasny et al., 2018), whereby the duration and magnitude of the parental exposure to OA could positively affect their offspring's responses.

Aquaculture facilities can be an invaluable partner to research and fisheries management institutions, particularly through their ability to supply fish of ecological, commercial, or recreational importance for experiments. Broodstock may reside in recirculating aquarium systems (RAS) — aquaria with limited water exchange and controlled water parameters that prevent the growth of wild water-borne pathogens. Broodstock respiration typically result in elevated pCO_2 within the RAS at levels comparable to, and in many cases, greatly exceeding OA projections (reviewed in Ellis et al., 2016). However, due to the difficulty of reliably attaining wild-caught larvae and the challenges involved in spawning and raising larvae, aquaculture facilities are often the sole provider of larval fish for experimental research.

The Hubbs-SeaWorld Research Institute (HSWRI) in Carlsbad (California, USA) is the primary hatchery contractor for California's Ocean Resources Enhancement and Hatchery Program (OREHP) administered by the California Department of Fish and Wildlife. In an effort to replenish natural populations, HSWRI has been breeding and rearing white seabass (*Atractoscion nobilis*) within RAS for release into the Southern California Bight since 1986 (Vojkovich and Crooke, 2001; Hervas et al., 2010). Broodstock and early life stages are maintained in RAS for environmental control and biosecurity before being moved into flow through systems and then acclimation cages prior to release as juveniles (Drawbridge et al., 2021). HSWRI is also a long-term collaborator with the Scripps Institution of Oceanography (SIO) at the University of California, San Diego, and this partnership has contributed to novel insights supporting early observations of the impacts of elevated pCO_2 on fish larvae (Checkley et al., 2009). Two studies demonstrated significantly larger otoliths in larval white seabass pre-

flexion larvae after exposure to 2500 μatm pCO_2 (Checkley et al., 2009a; Shen et al., 2016). However, exposure to elevated pCO_2 and the ensuing enlarged utricular otoliths did not significantly impact the larva's vestibular function (Shen et al., 2016). The intention of this study is to expand upon these morphological and behavioral observations through an exploration of other aspects of larval white seabass physiology.

In this study, we exposed larval white seabass to control pCO_2 (560 ± 32 μatm) and elevated pCO_2 reflective of projected OA conditions (1971 ± 55 μatm) during the first five days post-fertilization (dpf). We hypothesized that exposure to OA conditions would induce an upregulation in acid-base machinery and corresponding increase in energy consumption. We proposed these physiological changes would be evident in the analysis of the skin ionocytes, relative NKA abundance, rOCR, and total length. A retroactive analysis of HSWRI RAS seawater chemistry records offered insights into broodstock conditions, and provided critical parental life history context to further understand our findings.

Materials and Methods

Animal care and experimental procedures were approved by Institutional Animal Care and Use Committee at the University of California, San Diego under protocol S12161.

White seabass broodstock RAS conditions and egg collection

HSWRI routinely monitors and records broodstock RAS water conditions, including temperature every 15 minutes (RCK Controls; CA, USA), salinity and total alkalinity every week (Pinpoint®; American Marine, CT, USA, and HACH digital titrator (HACH, CO, USA), and O_2 and pH twice per day (HACH40d multimeter with LDO101 and PHC101 probes). Soda ash (Na_2CO_3) is added to RAS seawater as needed to maintain stable pH level as commonly performed by aquaculture facilities utilizing RAS. Seawater pCO_2 was calculated with CO2SYS

153 using the recorded temperature, salinity, pH, and total alkalinity data. The accuracy of HSWRI's
154 pH measurements was validated using the purified m-cresol purple method on discrete
155 seawater samples as described below.
156 Larvae were spawned from adult white seabass (12 males and 12 females; >61 cm and
157 >9.1 kg at the time of capture) that were captured in the wild between 2009 and 2012 and kept
158 within RAS at HSWRI. Spawning at HSWRI is induced through photothermal manipulation by
159 increasing 'daytime' duration from 10 to 14 hours, and by raising seawater temperature from
160 14°C to 18°C to mimic the warmer spawning season. Fertilization occurs within the RAS and
161 viable eggs float to the surface and are gently collected with a mesh at the outflow. In our study,
162 eggs were collected on three separate occasions (June 15, June 29, and July 28, 2016) for
163 three replicate experiments (EXP 1 – 3). For EXP 1, 2, and 3, the pH of the broodstock RAS at
164 the time of egg collection was 7.39, 7.39, and 7.53, respectively. Fertilized white seabass eggs
165 were transported to SIO within 12 hours post-fertilization for inspection and initiation of
166 experiments.
167
168 ***Experimental pCO_2 conditions***
169 White seabass eggs were observed using a light microscope; undamaged, fertilized
170 eggs were transferred into 5-L water-jacketed (18°C) glass vessels (400 eggs/vessel) and
171 larvae were reared until 5 dpf. The vessels contained filtered seawater continuously bubbled
172 with certified air-CO_2 gas mixture resulting in average pCO_2 of 560 ± 32 µatm and pH of 7.92 ±
173 0.02 (control), and pCO_2 of 1971 ± 55 µatm and pH of 7.42 ± 0.03 (OA-exposed) (Supp. Table
174 1). The experiment was repeated three times, with each experiment having three vessels per
175 treatment. High mortality was detected in one control and one OA-exposed vessel within EXP 3
176 for unknown reasons, and these two vessels were excluded from analysis.

177 At the end of the 5-day exposure, subsets of larvae were selected for microrespirometry
178 or euthanized with tricaine methanesulfonate (0.5 g l^{-1}) and processed for
179 immunohistochemistry or Western blotting. In EXP 1 and EXP 2, total length was measured
180 immediately after euthanasia under a dissection microscope. In EXP 3, 2 – 4 dpf larvae were
181 additionally sampled for total length measurements and immunohistochemistry.
182 At the end of each experiment, 250-mL seawater samples were collected from each
183 vessel and poisoned with 100 µL of mercuric chloride for inorganic carbon chemistry
184 measurements. A_T and dissolved inorganic carbon chemistry (DIC) were measured by the
185 Dickson laboratory (SIO) using open-cell potentiometric titration and coulometry, respectively.
186 The software CO_2Calc (Robbins et al., 2010) was used to estimate pH and pCO_2 from the
187 measured A_T and DIC.
188
189 ***Immunohistochemistry***
190 Larvae were fixed in 3% paraformaldehyde, 0.35% glutaraldehyde, 0.1 M cacodylate
191 buffer (catalog number: 15949; Electron Microscopy Sciences, Hatfield, PA, USA) for 4 hours at
192 room temperature, transferred to 50% ethanol overnight, and stored in 70% ethanol. Whole-
193 mount immunostaining was performed using the Vectastain® Universal HRP R.T.U. kit (Vector
194 Laboratories, Inc., Burlingame, CA, USA) following a previously described protocol (Kwan et al.,
195 2019b, a), and the α5 mouse monoclonal anti-NKA antibody (1.5 µg/mL) (Lebovitz et al., 1989)
196 (Developmental Studies Hybridoma Bank; Iowa University). This antibody is routinely used for
197 detecting NKA in fish (Melzner et al., 2009; Yang et al., 2013; Tang et al., 2014; Kwan et al.,
198 2019a, 2020).
199 Immunostained larvae were imaged on a Leica DMR compound microscope (Leica
200 Microsystems, Inc., Buffalo Grove, IL, USA) attached to a Canon Rebel T3i SLR camera and
201 processed as previously described in detail (Kwan et al., 2019b). Briefly, the images were focal-
202 stacked using Helicon Focus software (HeliconSoft, Kharkov, Ukraine) and stitched using

Adobe Photoshop CS6 (Adobe Systems, San Jose, USA). Ionocytes were identified by intense NKA-immunostaining. Relative ionocyte area (RIA) was calculated as the number of cutaneous ionocytes multiplied by their average area, and divided by the larva's surface area (Kwan et al., 2019a, b). Readers are referred to Kwan *et al.*, 2019b for further methodological details. Measurements were made using the freehand tool from FIJI (Schindelin et al., 2012) and a Wacom Intuos tablet (Saitama, Japan).

Western blotting

Larvae were flash frozen in liquid N_2 and stored at -80°C. Frozen larvae pooled from each vessel were pulverized in liquid N_2 by mortar and pestle, mixed in ice-cold homogenization buffer (250 mmol l^{-1} sucrose, 1 mmol l^{-1} EDTA, 30 mmol l^{-1} Tris, 10 mmol l^{-1} BHH, 1 mmol l^{-1} PMSF, 1 mmol l^{-1} DTT, pH 7.5), and centrifuged at 500 g for 10 min at 4°C to remove debris. The supernatant was saved ("crude homogenate"), and its total protein concentration was determined by Bradford Protein Assay. An additional sample that was not part of the experiments was designated as the standard and loaded into every gel to normalize results across immunoblots. Western blotting was performed as previously described (Kwan et al., 2019a, 2020), with 5 µg of total protein from each sample or standard loaded into a separate lane of the gels. The bands were imaged using the ChemiDoc™ MP system (Bio-Rad Laboratories, Inc., Hercules, CA, USA). The NKA antibody recognized a single band at the expected ~100 kDA (Supp. Fig. 2). Relative NKA abundance in each lane was quantified using Image Lab™ (Bio-Rad Laboratories, Inc.) and normalized relative to the standard.

Resting oxygen consumption rate

Larval resting O_2 consumption rate (rOCR) was measured using a Unisense MicroRespiration System and SensorTrace Rate software (Unisense A/S, Aarhus, Denmark). Ten larvae were removed from each vessel, and duplicate groups of five larvae were placed into

two 4-mL glass microrespiration chambers containing seawater from the respective vessel. The seawater in the microrespirometry chamber was maintained at 18°C by immersion into a water bath, and stirred at 600 rpm using a glass-embedded micromagnet. OCR measurements of groups of larvae are common given their small size (Cattano et al., 2016; Peck and Moyano, 2016).

After a 10 min acclimation period, O_2 concentration in the chamber was measured every second for 50 min. Larvae behavior was observed for 1 min every 15 min. Background microbial respiration rate was measured in chambers containing seawater only. The slope of the linear regression of O_2 concentration over time was taken as the rOCR for each group of five larvae. Duplicate measurements for each vessel were averaged and background microbial respiration was subtracted. The rOCR of an individual larva was estimated by dividing the group's rOCR by five. Statistical analyses were performed on these individual-based rOCR (μL O_2 ind^{-1} h^{-1}) estimates.

Data analysis

Statistical analyses were performed in GraphPad Prism (version 7.0a). Normality was assessed with the Shapiro-Wilks test. An alpha level of 0.05 was used for significance in all statistical tests. Linear regression was used to assess changes in RIA as a function of pCO_2 for larvae between 2 - 5 dpf. RIA, relative NKA abundance, rOCR, and total length were analyzed using two-tailed *t*-test. All experimental mean ± SEM, sample size, and statistical values are reported in Supp. Table 2.

Results

In EXP 1 and 2, we measured the total length of freshly-sacrificed 5 dpf larvae, and found that it was not significantly affected by OA exposure ($p = 0.6473$; Fig. 1A; Supp. Table 3). In EXP 3, we collected and fixed larvae between 2 and 5 dpf to investigate potential effects on

growth rate. Similarly, OA exposure did not affect the larval white seabass' growth rate (p = 0.4470; Fig. 1B; Supp. Table 4).

Immunostaining of 5 dpf larvae revealed the cutaneous NKA-rich ionocytes were concentrated on the anterior end of both control and OA-exposed larvae (Supp. Fig. 4). OA-exposed larvae had a significantly higher number of ionocytes than control larvae (p = 0.0410; Fig. 2A; Supp. Table 5). Since the total larva surface area was virtually identical between treatments (p > 0.9999; Supp. Table 5), OA-exposed larvae had a significantly higher ionocyte density compared to control larvae (p = 0.0008; Fig. 2B; Supp. Table 5). However, ionocytes of OA-exposed larvae tended to be smaller than those of control larvae (p = 0.0840; Fig. 2C; Supp. Table 5). As a result, there were no differences in RIA between the control and OA-exposed larvae at 5 dpf (p = 0.6129; Fig. 2D; Supp. Table 5) indicative of similar total cutaneous ion-transporting capacities. This result was in alignment with the Western blot analysis showing a lack of significant difference in NKA abundance between OA-exposed and control larvae (p = 0.2156; Fig. 2E; Supp. Fig. 2; Supp. Table 6). Similarly, the rate at which larval RIA decreased over the 2 to 5 dpf developmental period (Fig. 3) was not affected by OA exposure (p = 0.6855; Figure 2F; Supp. Table 4).

Throughout microrespiration trials from EXP 1 and 2, larvae from both treatments remained largely inactive during experiments, occasionally engaging in swimming bursts to re-orient themselves. We found oxygen declined linearly as a result of larval respiration, but there were no significant differences in rOCR between OA-exposed and control larvae (p = 0.928; Fig. 4; Supp. Table 7).

The lack of any major physiological differences between control larvae and those exposed to elevated pCO_2 led us to conduct a retrospective analysis of the broodstock RAS seawater chemistry. Records indicated that the parents of the larval white seabass used in our study were exposed to an average of ~1,200 µatm pCO_2 (pH ~7.6) at least 3.5 years prior to our experiment (Fig. 5A, B). The average total alkalinity, dissolved O_2 (DO), temperature, and

281 salinity was 2289 ± 23 μmol kg^{-1} SW^{-1}, 9.10 ± 0.05 mg/L, 15.9 ± 2.3 °C, and 33.65 ± 0.03 ppt,
282 respectively (Supp. Fig. 3). Furthermore, on the days the eggs were collected for our
283 experiments, the pH of the outflowing water was 7.39 (~2,073 ± 42 μatm), 7.36 (~2,236 ± 45
284 μatm), and 7.53 (~1,470 ± 15 μatm). Therefore, the RAS's pCO_2 levels are not only comparable
285 to predicted OA-levels for the year 2300, but also analogous to our larval white seabass'
286 experimental conditions.
287
288 **Discussion**
289 We hypothesized that exposure to elevated pCO_2 would increase the demand for ion-
290 transport to maintain acid-base homeostasis by white seabass larvae, which would be reflected
291 in higher RIA, NKA abundance, and rOCR. Contrary to our hypothesis, none of these variables
292 were significantly different between control and OA-exposed larvae. Additionally, we did not
293 detect differences in the growth parameters analyzed. Furthermore, our total length
294 measurements were consistent with two previous larval white seabass OA studies (Checkley et
295 al., 2009b; Shen et al., 2016), thereby ruling out developmental differences. Altogether, our
296 results indicate that white seabass larvae were able to cope with the elevated pCO_2 levels
297 without significant ion-regulatory adjustments or any major additional energetic cost.
298 Alternatively, the acid-base machinery and energetics of larval white seabass might have been
299 affected in ways that were not measured in our experiment. Additionally, it remains unclear
300 whether the chronic exposure to elevated pCO_2 within the broodstock tank could have had an
301 effect on the larva's physiology, for example, through natural selection or transgenerational
302 acclimation.
303 NKA is abundantly expressed in larval skin ionocytes, which allows for the identification
304 and quantification of these ion-transporting cells using whole larva immunohistochemistry.
305 Because NKA is the main driving force for ion-transport in marine fish, RIA and NKA abundance

306 serve as proxies for ion-transporting capacity and its underlying energy demand. Traditionally,
307 the ion-transporting capacity of fish larvae was estimated based on skin ionocyte density in a
308 specific area of the fish (Ayson et al., 1994; Hiroi et al., 1998, 1999; Varsamos et al., 2002). In
309 our experiment, skin ionocyte density in OA-exposed larvae was higher than in control larvae;
310 however, ion-transporting capacity also depends on ionocyte size. To address this issue, we
311 estimated RIA by measuring both ionocyte number and size as well as the surface area of the
312 entire immunostained larvae. In doing so, RIA is a more accurate proxy for ion-transporting
313 capacity than ionocyte density (Kwan et al., 2019a, b). Interestingly, OA-exposed larvae had
314 smaller average ionocyte size than control larvae. Although the difference in ionocyte size was
315 not statistically significant, it resulted in OA-exposed and control larvae having similar RIA.
316 Since these ionocytes have irregular shapes, we could not use simple math to calculate
317 ionocyte volume. Instead, we used Western blotting to quantify total NKA protein within whole
318 larvae as another proxy for ion-transporting capacity. This approach revealed lower total NKA
319 abundance in OA-exposed larvae compared to control larvae, but the difference was not
320 statistically significant. Taken together, our results suggest that the ion-transporting capacities of
321 OA-exposed and control larvae are similar, and that the observed differences in some of the
322 parameters were due to inherent variability of the larvae and techniques.
323 Estimation of ion-transport capacity by immunodetecting NKA via immunohistochemistry
324 and Western blotting is a powerful approach because it considers both the number and size of
325 ionocytes in relation to larval size, as well as total NKA protein abundance. Since NKA is the
326 most ATP-demanding step of ion-transport, NKA abundance serves as a proxy for energy
327 utilization. However, the quantification of NKA abundance has various limitations that must be
328 considered. In addition to H^+ excretion, the marine fish's NKA-rich ionocyte is also used for NaCl
329 excretion to maintain nominal blood osmolarity, and presumably also NH_4^+ excretion and Ca^{2+}
330 homeostasis (reviewed in Evans et al., 2005; Glover et al., 2013). Therefore, a putative increase
331 in NKA abundance to upregulate H^+ excretion may not be detectable given the relatively high

baseline levels from existing multi-functional physiological roles of the NKA-rich ionocyte. Furthermore, larval fishes grow at a very fast rate (Finn and Kapoor, 2008), and their rapidly metabolizing tissue determine rOCRs that are 50-80% higher than that of juveniles and adults (Post and Lee, 1996). As a result, the proportionally higher CO_2 production in larval fish coupled with their high reliance on ammonia-producing amino-acid catabolism (Finn et al., 2002) could entail an intrinsically high capacity for acid-base regulation that is sufficient to cope with the effects of OA without any major adjustments in NKA abundance or rOCR. Alternatively, the putative upregulation of H^+ excretion could have been achieved by increasing the abundance of other ion-transporting proteins such as Na^+/H^+ exchangers, Na^+/HCO_3^- cotransporters, and carbonic anhydrases that were not measured in our experiment.

The significant increase in protein biosynthesis or turnover rate should have been reflected in the rOCR measurements. For example, sea urchin and oyster larvae exposed to comparable pCO_2 levels demonstrated both increased rOCR and protein turnover rates (Pan et al., 2015; Frieder et al., 2018). Alternatively, while we did not find evidence of increased protein biosynthesis, OA may have affected metabolic energy allocation. Since 5 dpf white seabass larvae still completely rely on their yolk sacs as their energy source (Moser et al., 1983), the allocation of energy towards protein biosynthesis would reduce the amount of energy available for other processes. Further studies examining protein biosynthesis are necessary to better understand the energetic responses of larval fishes to OA, which could be especially important in the presence of other stressors that impose additional energetic demand.

The retroactive analysis of HSWRI broodstock RAS conditions revealed an average $pCO_{2\ of}$ ~1,200 µatm during the 3.5 years prior to our experiments, and occasionally approached ~3,000 µatm. As a consequence, the broodstock fish were chronically acclimated to elevated pCO_2 levels comparable to OA conditions predicted for the next century (Caldeira and Wickett, 2003, 2005; Goodwin et al., 2018; Bindoff et al., 2019). This raises the question of whether transgenerational acclimation influenced the larval white seabass physiology within our study,

358 and possibly contributing to the lack of significant differences between OA-exposed and control
359 larvae. There is growing evidence indicating parental exposure to a given stressor may enhance
360 offspring performance (reviewed in Donelson et al., 2018). Some possibilities include the
361 maternal transmission of more efficient mitochondria [as proposed for Three-Spine Stickleback
362 (*Gasterosteus aculeatus*) under thermal stress (Shama et al., 2014)] and of enhanced non-
363 bicarbonate buffering capacity [(suggested for Atlantic Cod (*Gadus morhua*) embryos (Dahlke *et*
364 *al*., 2020)], and epigenetic modulation [as proposed for Spiny Damselfish (*Acanthochromis*
365 *polyacanthus*) exposed to OA (Schunter et al., 2018)]. Interestingly, white seabass spawning,
366 fertilization, and early embryo development also occur within the HSWRI RAS, and thus
367 gametes and embryos are exposed to elevated pCO_2 during these crucial life stages. This
368 suggests the possibilities of natural selection and developmental plasticity resulting in OA-
369 resilient gametes, embryos, and larvae. Interestingly, if these effects indeed existed, the release
370 of juveniles through OREHP (Vojkovich and Crooke, 2001; California Department of Fish and
371 Game, 2002; Hervas et al., 2010) into the local ecosystem could be an example of an assisted
372 evolution strategy similar to that proposed for coral reef resiliency (Van Oppen et al., 2015).
373 However, studying parental effects, developmental plasticity, and transgenerational
374 mechanisms require a stringent experimental design (Donelson et al., 2018). Since our study
375 was not designed to answer these questions, it cannot discern whether the broodstock's chronic
376 exposure to elevated pCO_2 had any effect on larval fitness. Nevertheless, the results presented
377 here present a useful blueprint for future experiments, which, in addition to white seabass larvae
378 from parental broodstock chronically acclimated to elevated pCO_2, must include larvae from
379 broodstock acclimated to past- or present-day CO_2 levels (the "environmental" and "ambient"
380 controls discussed in Donelson *et al*. (2018). These types of studies will not be trivial due to the
381 challenges associated with maintaining broodstock fish at different CO_2 levels during extended
382 periods of time, achieving spawning, and rearing larvae. Performing these studies are further
383 complicated by the relatively short duration of research funding schemes, student programs,

and postdoctoral researcher contracts. With this in mind, it will remain crucial to continue to foster partnerships between academia and aquaculture facilities, which will allow to tackle essential questions that require extended experimentation periods such as transgenerational acclimation.

In conclusion, the lack of differences in RIA, NKA abundance, rOCR, and length obtained in the current study indicates that White Seabass larvae are able to cope with OA without major alterations in ion-transporting capacity, energy consumption, or growth when exposed to elevated pCO_2 (~2000 μatm) projected for the next century. However, in-depth analyses provided hints for potential novel effects such as changes in ionocyte size, and helped identify the need for more detailed studies about the basic physiology of marine fish larvae, their energy allocation in response to OA and multi-stressors, and the potential for transgenerational acclimation through parental effects, developmental plasticity, and natural selection. This highlights the difficulty of ascribing potential effects of OA on marine organisms based on acute laboratory studies. Finally, we would like to emphasize the importance of collaborations with aquaculture facilities, such as HSWRI, to continue advancing our understanding on the impacts of OA on fish.

Competing interests

No competing interests declared.

Author contributions

S.G.S., G.T.K, M.T., and D.M.C. designed research; S.G.S. and G.T.K. performed research; S.G.S., G.T.K., and M.T. analyzed results and wrote the manuscript. M.D. provided historical data on white seabass broodstock holding conditions. D.M.C and M.D. provided guidance and reviewed draft manuscripts. All authors gave final approval for publication.

Acknowledgements

GTK was funded by the San Diego Fellowship, NSF GRFP, and the NSF Postdoctoral Research Fellowship in Biology (award: 1907334). SGS was funded by the National Science Foundation (NSF) Graduate Research Fellowship Program (GRFP). We thank Erica Bromby-Fanning, Eric McIntire, Sabrina Sobel, Christy Varga, and other personnel at HSWRI for providing fertilized white seabass eggs and seawater data. HSWRI's contributions were made possible by the OREHP that funds this portion of the hatchery operations. We are grateful to Dr. Lauren Linsmayer and to Dr. Greg Rouse (SIO) for assisting in the microrespiration experiments and loan of the microscope and camera system, respectively. We appreciate Dr. Andrew Dickson and Dr. David Cervantes for general guidance and seawater chemistry analysis.

Data availability

All data are available in our supplemental materials.

References

Ayson FG, Kaneko T, Hasegawa S, Hirano T (1994) Development of mitochondrion-rich cells in the yolk-sac membrane of embryos and larvae of tilapia, *Oreochromis mossambicus*, in fresh water and seawater. J Exp Zool 270:129–135. doi: 10.1002/jez.1402700202

Baumann H, Talmage SC, Gobler CJ (2012) Reduced early life growth and survival in a fish in direct response to increased carbon dioxide. Nat Clim Chang 2:38–41. doi: 10.1038/nclimate1291

Beaugrand G, Brander KM, Lindley JA, et al (2003) Plankton effect on cod recruitment. Nature 426:661–664.

Bignami S, Sponaugle S, Cowen RK (2013) Response to ocean acidification in larvae of a large tropical marine fish, *Rachycentron canadum*. Glob Chang Biol 19:996–1006. doi: 10.1111/gcb.12133

Bindoff NL, Cheung WWL, Kairo JG, et al (2019) Changing Ocean, Marine Ecosystems, and Dependent Communities. IPCC Spec Rep Ocean Cryosph a Chang Clim 447–588.

Caldeira K, Wickett ME (2003) Oceanography: anthropogenic carbon and ocean pH. Nature 425:365. doi: 10.1038/425365a

Caldeira K, Wickett ME (2005) Ocean model predictions of chemistry changes from carbon dioxide emissions to the atmosphere and ocean. J Geophys Res C-Oceans 110:12 pp.-12 pp. doi: 10.1029/2004jc002671

Cattano C, Giomi F, Milazzo M (2016) Effects of ocean acidification on embryonic respiration

445 and development of a temperate wrasse living along a natural CO2 gradient. Conserv
446 Physiol 4:1–10. doi: 10.1093/conphys/cov073
447 CDFG (2002) White seabass fishery management plan (WSFMP). Los Alamitos
448 Checkley DM, Dickson AG, Takahashi M, et al (2009a) Elevated CO2 Enhances Otolith Growth
449 in Young Fish: Supplemental Material. Science (80-) 324:1683–1683. doi:
450 10.1126/science.1169806
451 Checkley DM, Dickson AG, Takahashi M, et al (2009b) Elevated CO2 enhances otolith growth
452 in young fish. Science 324:1683. doi: 10.1126/science.1169806
453 Dahlke FT, Leo E, Mark FC, et al (2017) Effects of ocean acidification increase embryonic
454 sensitivity to thermal extremes in Atlantic cod, *Gadus morhua*. Glob Chang Biol 23:1499–
455 1510. doi: 10.1111/gcb.13527
456 Dahlke FT, Lucassen M, Bickmeyer U, et al (2020) Fish embryo vulnerability to combined
457 acidification and warming coincides with a low capacity for homeostatic regulation. J Exp
458 Biol 223:jeb212589. doi: 10.1242/jeb.212589
459 Donelson JM, Salinas S, Munday PL, Shama LNS (2018) Transgenerational plasticity and
460 climate change experiments: Where do we go from here? Glob Chang Biol 24:13–34. doi:
461 10.1111/gcb.13903
462 Drawbridge M, Shane M, Silbernagel C (2021) The status of white seabass, *Atractoscion nobilis*
463 as a commercially ready species for marine US aquaculture. J World Aquac Soc 1–15. doi:
464 10.1111/jwas.12772
465 Ellis RP, Urbina MA, Wilson RW (2016) Lessons from two high CO_2 worlds - future oceans and
466 intensive aquaculture. Glob Chang Biol 2100:1–8. doi: 10.1111/gcb.13515
467 Esbaugh AJ (2017) Physiological implications of ocean acidification for marine fish: emerging
468 patterns and new insights. J Comp Physiol B 0:0. doi: 10.1007/s00360-017-1105-6
469 Evans DH, Piermarini PM, Choe KP (2005) The Multifunctional Fish Gill: Dominant Site of Gas
470 Exchange, Osmoregulation, Acid-Base Regulation, and Excretion of Nitrogenous Waste.
471 Physiol Rev 85:97–177. doi: 10.1152/physrev.00050.2003
472 Finn RN, Rønnestad I, Van der Meeren T, Fyhn HJ (2002) Fuel and metabolic scaling during
473 the early life stages of Atlantic cod *Gadus morhua*. Mar Ecol Prog Ser 243:217–234. doi:
474 10.3354/meps243217
475 Finn RN, Kapoor B (2008) Fish Larval Physiology.
476 Flynn EE, Bjelde BE, Miller NA, Todgham AE (2015) Ocean acidification exerts negative effects
477 during warming conditions in a developing Antarctic fish. Conserv Physiol 3:1–16. doi:
478 10.1093/conphys/cov033
479 Frieder CA, Applebaum SL, Pan TCF, Manahan DT (2018) Shifting balance of protein synthesis
480 and degradation sets a threshold for larval growth under environmental stress. Biol Bull
481 234:45–57. doi: 10.1086/696830
482 Frommel AY, Maneja R, Lowe D, et al (2011) Severe tissue damage in Atlantic cod larvae under
483 increasing ocean acidification. Nat Clim Chang 2:42–46. doi: 10.1038/nclimate1324
484 Glover CN, Bucking C, Wood CM (2013) The skin of fish as a transport epithelium: A review. J
485 Comp Physiol B Biochem Syst Environ Physiol 183:877–891. doi: 10.1007/s00360-013-
486 0761-4
487 Goodwin P, Brown S, Haigh ID, et al (2018) Adjusting Mitigation Pathways to Stabilize Climate
488 at 1.5°C and 2.0°C Rise in Global Temperatures to Year 2300. Earth's Futur 6:601–615.
489 doi: 10.1002/2017EF000732
490 Hervas S, Lorenzen K, Shane MA, Drawbridge MA (2010) Quantitative assessment of a white
491 seabass (*Atractoscion nobilis*) stock enhancement program in California: Post-release
492 dispersal, growth and survival. Fish Res 105:237–243. doi: 10.1016/j.fishres.2010.06.001
493 Heuer RM, Grosell M (2014) Physiological impacts of elevated carbon dioxide and ocean
494 acidification on fish. AJP Regul Integr Comp Physiol 307:R1061–R1084. doi:
495 10.1152/ajpregu.00064.2014

Hiroi J, Kaneko T, Seikai T, Tanaka M (1998) Developmental sequence of chloride cells in the body skin and gills of Japanese Flounder (*Paralichthys olivaceus*) larvae. Zoolog Sci 15:455–60. doi: 10.2108/0289-0003(1998)15[455:DSOCCI]2.0.CO;2

Hiroi J, Kaneko T, Tanaka M (1999) In vivo sequential changes in chloride cell morphology in the yolk-sac membrane of Mozambique tilapia (*Oreochromis mossambicus*) embyros and larvae during seawater adaptation. J Exp Biol 202:3485–3495.

Hjort J (1926) Fluctuations in the year classes of important food fishes. J Cons int Explor Mer 1:5–38.

Houde ED (2009) Recruitment variability. In: Fish Reproductive Biology: Implications for Assessment and Management. Wiley-Blackwell, West Sussex, pp 91–171

Ishimatsu A, Hayashi M, Kikkawa T (2008) Fishes in high-CO2, acidified oceans. Mar Ecol Prog Ser 373:295–302. doi: 10.3354/meps07823

Kwan GT, Wexler JB, Wegner NC, Tresguerres M (2019a) Ontogenetic changes in cutaneous and branchial ionocytes and morphology in yellowfin tuna (*Thunnus albacares*) larvae. J Comp Physiol B Biochem Syst Environ Physiol 189:81–95. doi: 10.1007/s00360-018-1187-9

Kwan GT, Finnerty SH, Wegner NC, Tresguerres M (2019b) Quantification of Cutaneous Ionocytes in Small Aquatic Organisms. Bio-protocol 9:e3227. doi: 10.21769/BioProtoc.3227

Kwan GT, Smith TR, Tresguerres M (2020) Immunological characterization of two types of ionocytes in the inner ear epithelium of Pacific Chub Mackerel (*Scomber japonicus*). J Comp Physiol B 190:419–431. doi: 10.1007/s00360-020-01276-3

Lebovitz RM, Takeyasu K, Fambrough DM (1989) Molecular characterization and expression of the (Na+ + K+)-ATPase alpha-subunit in *Drosophila melanogaster*. EMBO J 8:193–202.

Meehl GA, Stocker TF, Collins WD, et al (2007) 2007: Global climate projections. In: Climate Change 2007: Contribution of Working Group I to the Fourth Assessment Report of the Intergovernmental Panel on Climate Change. Cambridge University Press, Cambridge, UK, pp 747–846

Melzner F, Gutowska M a., Langenbuch M, et al (2009) Physiological basis for high CO_2 tolerance in marine ectothermic animals: pre-adaptation through lifestyle and ontogeny? Biogeosciences Discuss 6:4693–4738. doi: 10.5194/bgd-6-4693-2009

Miller GM, Watson SA, Donelson JM, et al (2012) Parental environment mediates impacts of increased carbon dioxide on a coral reef fish. Nat Clim Chang 2:858–861. doi: 10.1038/nclimate1599

Moser GH, Ambrose DA, Busby MS, et al (1983) Description of early stages of white seabass, *Atractoscion nobilis*, with notes on distribution. CalCOFI Rep 24:182–193.

Munday PL, Donelson JM, Dixson DL, Endo GGK (2009) Effects of ocean acidification on the early life history of a tropical marine fish. Proc R Soc B Biol Sci 276:3275–3283. doi: 10.1098/rspb.2009.0784

Munday PL (2014) Transgenerational acclimation of fishes to climate change and ocean acidification. F1000Prime Rep 6:1–7. doi: 10.12703/P6-99

Munday PL, Watson S-A, Parsons DM, et al (2016) Effects of elevated CO2 on early life history development of the yellowtail kingfish, *Seriola lalandi*, a large pelagic fish. ICES J Mar Sci J du Cons 73:641–649. doi: 10.1093/icesjms/fsv210

Murray C, Malvezzi A, Gobler C, Baumann H (2014) Offspring sensitivity to ocean acidification changes seasonally in a coastal marine fish. Mar Ecol Prog Ser 504:1–11. doi: 10.3354/meps10791

Murray CS, Fuiman LA, Baumann H (2016) Consequences of elevated CO2 exposure across multiple life stages in a coastal forage fish. ICES J Mar Sci J du Cons fsw179. doi: 10.1093/icesjms/fsw179

Pan TCF, Applebaum SL, Manahan DT (2015) Experimental ocean acidification alters the allocation of metabolic energy. Proc Natl Acad Sci U S A 112:4696–4701. doi:

10.1073/pnas.1416967112
Peck MA, Moyano M (2016) Measuring respiration rates in marine fish larvae: Challenges and advances. J Fish Biol 88:173–205. doi: 10.1111/jfb.12810
Pimentel MS, Faleiro F, Dionisio G, et al (2014) Defective skeletogenesis and oversized otoliths in fish early stages in a changing ocean. J Exp Biol 217:2062–2070. doi: 10.1242/jeb.092635
Pimentel MS, Faleiro F, Diniz M, et al (2015) Oxidative Stress and Digestive Enzyme Activity of Flatfish Larvae in a Changing Ocean. PLoS One 10:e0134082. doi: 10.1371/journal.pone.0134082
Post J, Lee J (1996) Metabolic ontogeny of teleost fishes. Can J Fish Aquat Sci 53:910–923. doi: 10.1139/f95-278
Robbins L, Hansen M, Kleypas J, Meylan S (2010) CO2Calc - A user-friendly seawater carbon calculator for Windows, Max OS X, and iOS (iPhone). 1–17.
Rossi T, Nagelkerken I, Simpson SD, et al (2015) Ocean acidification boosts larval fish development but reduces the window of opportunity for successful settlement. Proc R Soc B Biol Sci 282:20151954. doi: 10.1098/rspb.2015.1954
Schindelin J, Arganda-Carreras I, Frise E, et al (2012) Fiji: an open-source platform for biological-image analysis. Nat Methods 9:676–682. doi: 10.1038/nmeth.2019
Schunter C, Welch MJ, Nilsson GE, et al (2018) An interplay between plasticity and parental phenotype determines impacts of ocean acidification on a reef fish. Nat Ecol Evol 2:334–342. doi: 10.1038/s41559-017-0428-8
Shama LNS, Strobel A, Mark FC, Wegner KM (2014) Transgenerational plasticity in marine sticklebacks: Maternal effects mediate impacts of a warming ocean. Funct Ecol 28:1482–1493. doi: 10.1111/1365-2435.12280
Shen SG, Chen F, Schoppik DE, Checkley DM (2016) Otolith size and the vestibulo-ocular reflex of larvae of white seabass *Atractoscion nobilis* at high pCO2. Mar Ecol Prog Ser 553:173–182. doi: 10.3354/meps11791
Stiasny MH, Mittermayer FH, Göttler G, et al (2018) Effects of parental acclimation and energy limitation in response to high CO2 exposure in Atlantic cod. Sci Rep 1–8. doi: 10.1038/s41598-018-26711-y
Tang CH, Leu MY, Yang WK, Tsai SC (2014) Exploration of the mechanisms of protein quality control and osmoregulation in gills of *Chromis viridis* in response to reduced salinity. Fish Physiol Biochem 40:1533–1546. doi: 10.1007/s10695-014-9946-3
Tresguerres M, Hamilton TJ (2017) Acid-base physiology, neurobiology and behaviour in relation to CO2 -induced ocean acidification. J Exp Biol 220:2136–2148. doi: 10.1242/jeb.144113
Van Oppen MJH, Oliver JK, Putnam HM, Gates RD (2015) Building coral reef resilience through assisted evolution. Proc Natl Acad Sci U S A 112:2307–2313. doi: 10.1073/pnas.1422301112
Varsamos S, Diaz J, Charmantier G, et al (2002) Location and morphology of chloride cells during the post-embryonic development of the European sea bass, *Dicentrarchus labrax*. Anat Embryol (Berl) 205:203–213. doi: 10.1007/s00429-002-0231-3
Vojkovich M, Crooke S (2001) White Seabass. In: California's living resources: a status report. Cal Fish Game, Sacramento, pp 206–208
Yang W, Kang C, Chang C, et al (2013) Expression Profiles of Branchial FXYD Proteins in the Brackish Medaka *Oryzias dancena*: A Potential Saltwater Fish Model for Studies of Osmoregulation. doi: 10.1371/journal.pone.0055470

Figures and Tables

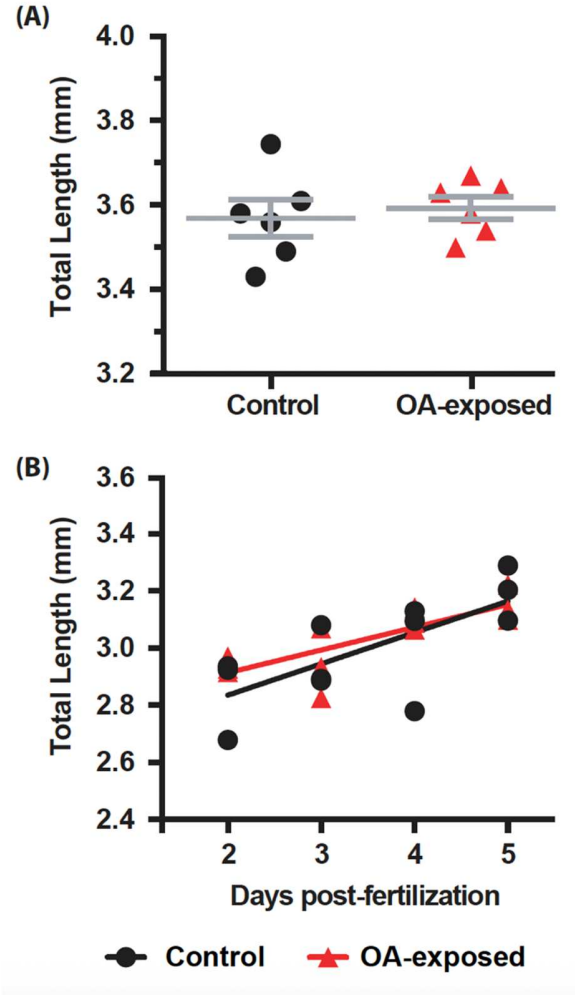

Figure 1. Total length of experimental larval white seabass. Control (black) and OA-exposed (red) larvae's (A) total length at 5 days post-fertilization ($t(10) = 0.4717$; $p = 0.6473$), and (B) over the 2 to 5 days post-fertilization ($F(1,20) = 0.6512$; $p = 0.4292$) were not significantly different. Data are presented as means ± S.E.M.

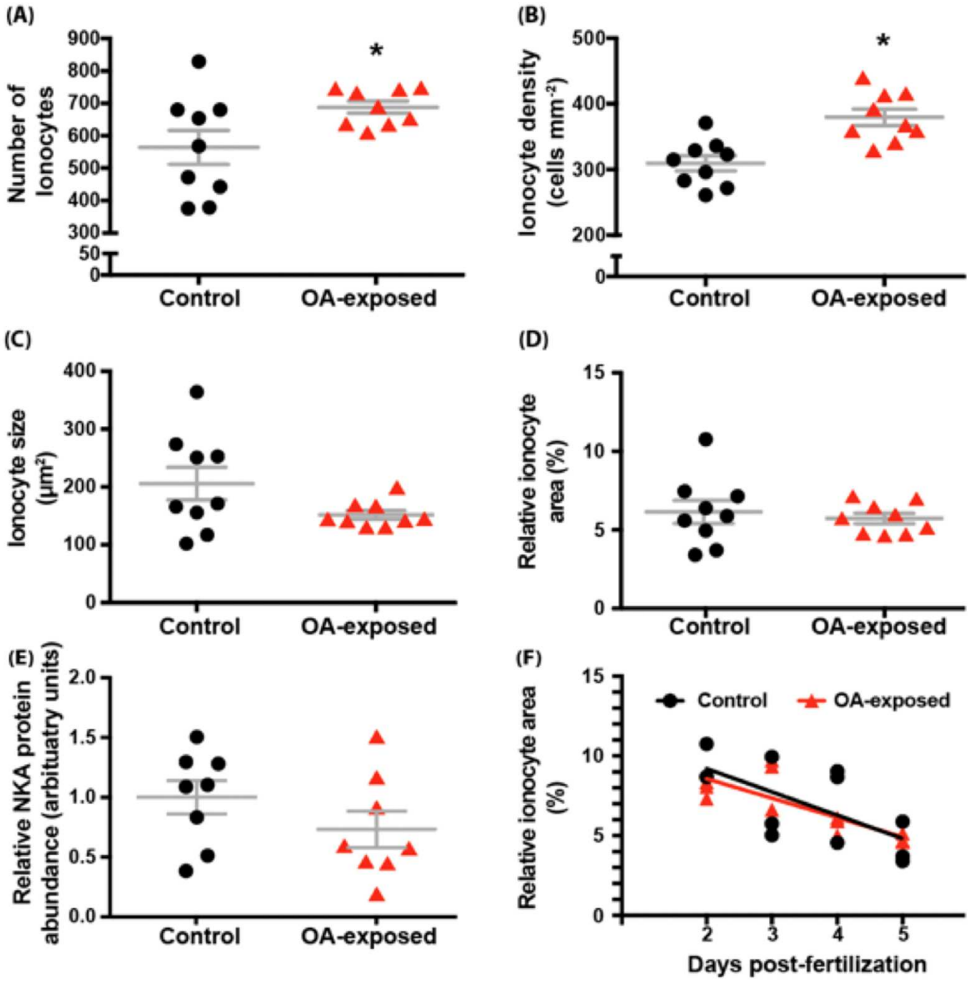

603

604 **Figure 2. Physiological responses of white seabass larvae exposed to control or OA**
605 **conditions.** The (A) number of ionocytes ($t(16) = 2.223$; $p = 0.0410$), (B) ionocyte density ($t(16)$
606 $= 4.106$; $p = 0.0008$), (C) ionocyte size ($t(16) = 1.843$; $p = 0.0840$), (D) relative ionocyte area
607 ($t(16) = 0.5161$; $p = 0.6129$), and (E) relative Na^+/K^+-ATPase abundance ($t(14) = 1.297$; $p =$
608 0.2156) of 5 days post-fertilization larvae exposed to control (black) or OA (red) conditions. (F)
609 The relative ionocyte area of larval white seabass over 2 to 5 days post-fertilization ($(1,20) =$
610 0.1689; $p = 0.6855$). Asterisks indicate significance at an alpha level of 0.05. Data are
611 presented as means ± S.E.M.

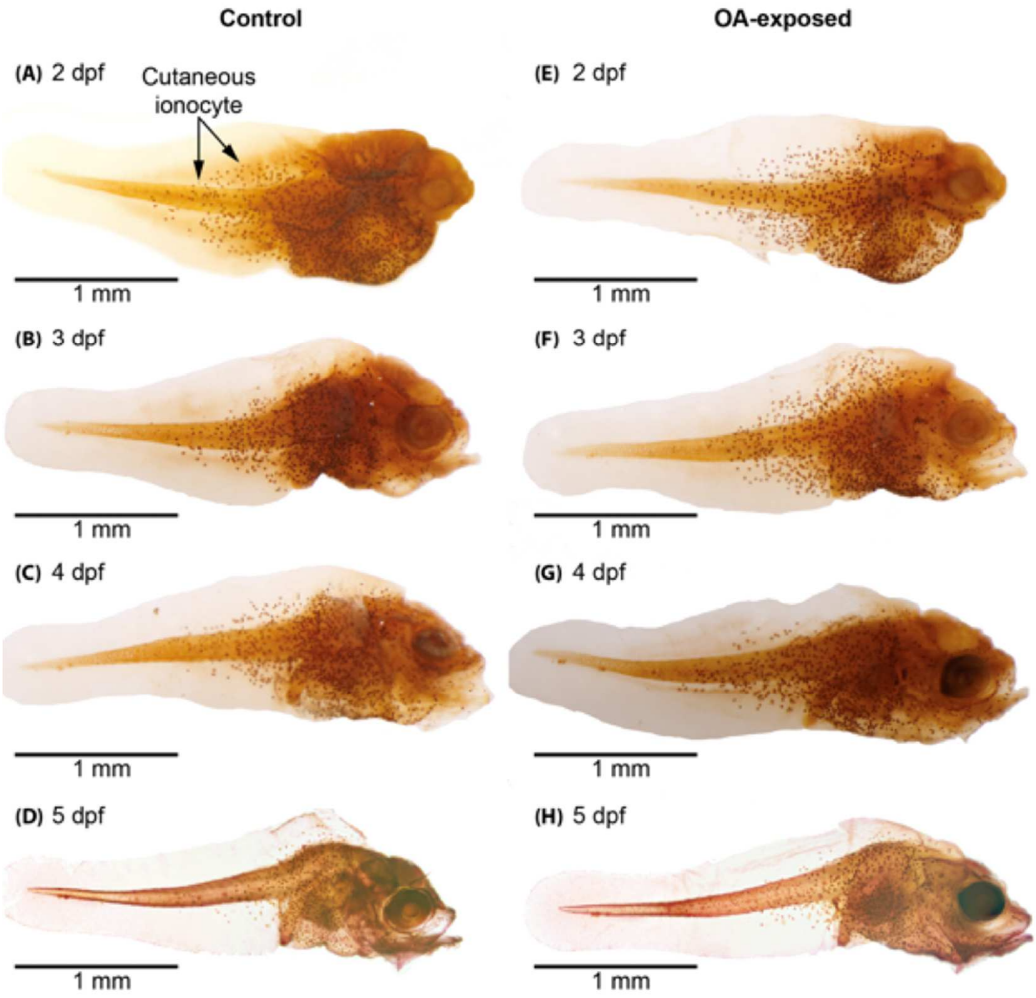

612

613 **Figure 3. Cutaneous ionocytes in white seabass larvae exposed to control or OA**

614 **conditions.** Representative images showing Na^+/K^+-ATPase immunostained cutaneous

615 ionocytes in larvae. (A-D) control treatment; (E-H) OA-exposed treatment; dpf = days post-

616 fertilization.

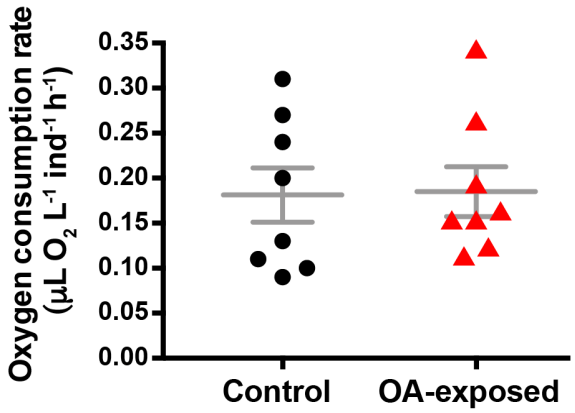

Figure 4. Oxygen consumption rates of white seabass larvae. The oxygen consumption rate of white seabass larvae (in groups of 5) from EXP 1 were measured over a 50-minute period and shown as a function of time. No significant differences in oxygen consumption rate were detected between the larvae reared in control (black) and those reared in OA-exposed (red) treatment ($t(14) = 0.0918$; $p = 0.928$). Data are presented as means ± S.E.M.

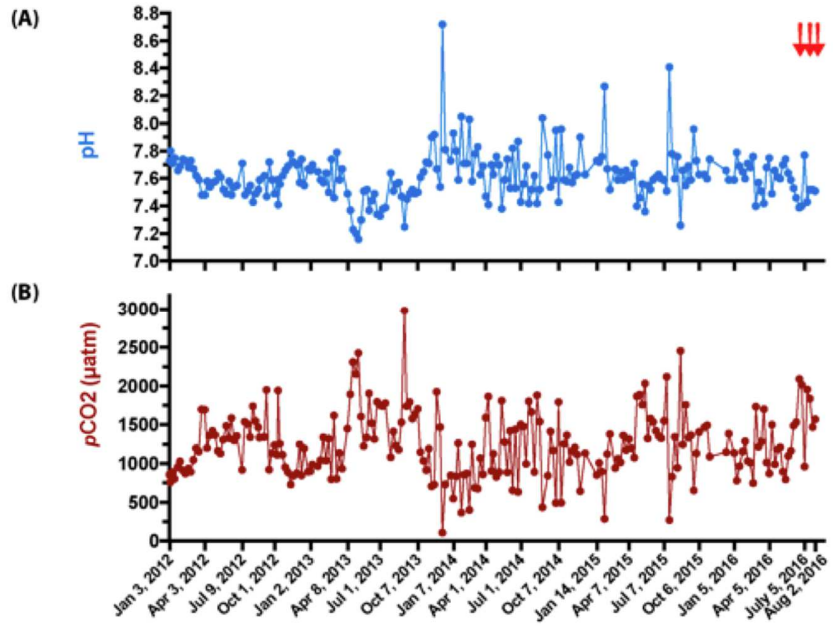

Figure 5. Water chemistry of the white seabass broodstock tank in the 3.5 years previous to larval collection. (A) pH and (B) pCO_2. Red arrows on the top right indicate the date of egg collections.

Larval skin ionocytes were identified by immunolabeling Na^+/K^+-ATPase (NKA)

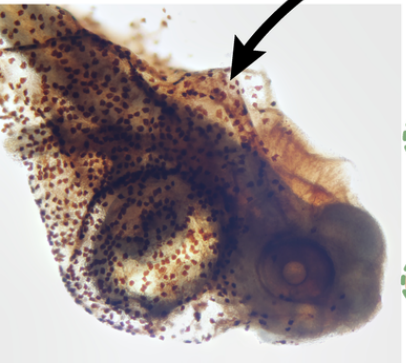

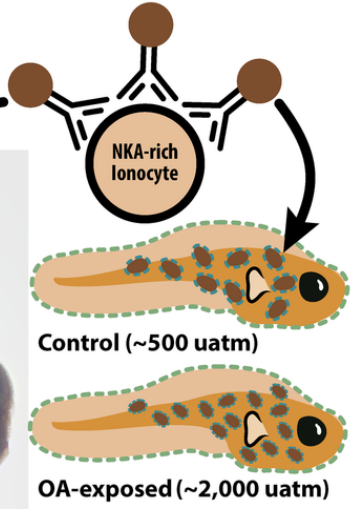

$$\text{Relative Ionocyte Area} = \frac{\text{Ionocyte Count} \times \text{Ionocyte Size}}{\text{Larval Surface Area}}$$

Ionocyte Count	Ionocyte Size	Larval Surface Area	Relative Ionocyte Area	Resting O_2 Consumption Rate	Total Length
Less	Larger	=	=	=	=
More	Smaller	=	=	=	=